Aqueous Humor Analysis Identifies Higher Branched Chain Amino Acid Metabolism as a Marker for Human Leukocyte Antigen-B27 Acute Anterior Uveitis and Disease Activity

FLEURIEKE H. VERHAGEN, EDWIN C.A. STIGTER, MIA L. PRAS-RAVES, BOUDEWIJN M.T. BURGERING, SASKIA M. IMHOF, TIMOTHY R.D.J. RADSTAKE, JOKE H. DE BOER, AND JONAS J.W. KUIPER

• PURPOSE: **Human leukocyte antigen-B27 (HLA-B27)–positive acute anterior uveitis (AAU) has a higher recurrence rate and shows more anterior chamber cell infiltration compared with HLA-B27–negative patients, suggesting distinct etiologies of these clinically overlapping conditions. To advance our understanding of the biology of AAU, we characterized the metabolic profile of aqueous humor (AqH) of patients with HLA-B27–associated AAU (B27-AAU) and noninfectious idiopathic AAU (idiopathic AAU).**

• DESIGN: **Experimental laboratory study.**

• METHODS: **AqH samples from 2 independent cohorts totaling 30 patients with B27-AAU, 16 patients with idiopathic AAU, and 20 patients with cataracts underwent 2 individual rounds of direct infusion mass spectrometry. Features predicted by direct infusion mass spectrometry that facilitated maximum separation between the disease groups in regression models were validated by liquid chromatography/tandem mass spectrometry–based quantification with appropriate standards.**

• RESULTS: **Partial least square-discriminant analysis revealed metabolite profiles that were able to separate patients with B27-AAU from those with iodiopathic AAU. Pathway enrichment analysis, based on metabolites on which separation of the groups in the partial least square-discriminant analysis model was based, demonstrated the involvement of branched-chain amino acid biosynthesis, ascorbate and aldarate metabolism, the tricarboxylic acid cycle, and glycolysis-diverting pathways (eg, serine biosynthesis) across all investigated cohorts. Notably, the metabolite ketoleucine was elevated in B27-AAU across all 3 runs and moderately—but robustly—correlated with anterior chamber cell count (correlation coefficient range 0.41–0.81).**

• CONCLUSIONS: **These results illustrate metabolic heterogeneity between HLA-B27–positive and HLA-B27–negative AAU, including an increase of branched-chain amino acid biosynthesis, that reflects disease activity in AAU. (Am J Ophthalmol 2019;198:97–110. © 2018 Elsevier Inc. All rights reserved.)**

ACUTE ANTERIOR UVEITIS (AAU) IS THE MOST COMMON form of uveitis. The presence or absence of the major histocompatibility complex class I allele human leukocyte antigen-B27 (HLA-B27) in patients with AAU is essential to classify patients into HLA-B27–positive (10%–88% of AAU, depending on geographic location and secondary or tertiary setting) or HLA-B27–negative idiopathic AAU.[1–3] HLA-B27–associated AAU (B27-AAU) and HLA-B27–negative idiopathic AAU share most clinical features, including a relatively favorable visual prognosis.[4] However, patients with B27-AAU generally have a younger age of onset, a more recurrent disease course, and generally have more marked anterior chamber cell infiltration.[5,6] In addition, B27-AAU is often accompanied by systemic rheumatic diseases, primarily ankylosing spondylitis (AS).[7] The genetic association with HLA-B27 and distinct disease evolution collectively hints toward a unique underlying biology for B27-AAU over idiopathic AAU. Yet to date, investigations of aqueous humor in B27-AAU and idiopathic AAU have mostly revealed shared molecular characteristics.[8,9]

Metabolomics refers to the detection and quantification of a broad range of small metabolic products (ie, metabolites) using mass spectrometry or nuclear magnetic resonance spectroscopy to map the complex biochemistry and cellular physiology of biological samples. This rapidly emerging field is commonly used to detect disease-specific metabolic signatures to better understand pathophysiology or to aid in diagnosis and reveal prognostic biomarkers.[10] Related studies in noninfectious uveitis have already revealed changes in the metabolic composition of vitreous humor and plasma of various uveitis types.[11,12]

AJO.com Supplemental Material available at AJO.com.

Accepted for publication Oct 1, 2018.

From the Ophthalmo-Immunology Unit (F.H.V., T.R.D.J.R., J.H.d.B., J.J.W.K.), Department of Ophthalmology (F.H.V., S.M.I., J.H.d.B., J.J.W.K.), Laboratory of Translational Immunology (F.H.V., T.R.D.J.R., J.J.W.K.), Department Molecular Cancer Research (E.C.A.S., M.L.P-R., B.M.T.B., T.R.D.J.R., J.H.d.B.), Section of Metabolic Diseases, and the Department of Rheumatology and Clinical Immunology (T.R.D.J.R.), University Medical Center Utrecht, Utrecht, the Netherlands.

Inquiries to: Fleurieke H. Verhagen, Department of Ophthalmology, University Medical Center Utrecht, Room B03.2.30, Heidelberglaan 100, 3584CX Utrecht, The Netherlands; e-mail: F.H.Verhagen@umcutrecht.nl

0002-9394/$36.00
https://doi.org/10.1016/j.ajo.2018.10.004

TABLE 1. Study cohorts

	B27-AAU	Idiopathic AAU	*P* Value	CAT
Discovery cohort (DIMS1)				
N	15	8		12
Male gender, %	60	13	.07[a]	25%
Mean age, y (SD)	44.6 (15.5)	55.0 (11.6)	.13[b]	69.6 (7.9)
Medication, n (%)				
Topical steroids	13 (87)	6 (75)	.59[a]	
Periocular steroids <3 months	4 (27)	1 (13)	.62[a]	
Systemic steroids	3 (20)	2 (25)	1.00[a]	
DMARDS or biologicals	1 (7)	1 (13)	1.00[a]	
Anterior chamber cell count, n (%)				
0	2 (13)	4 (50)		NA
0.5+	3 (20)	1 (13)		NA
1+	3 (20)	1 (13)		NA
2+	5 (33)	1 (13)		NA
3+	2 (13)	0		NA
4+	0	0		NA
Hypopyon	0	1 (13)		NA
Mean storage time, months (range)	58 (20–114)	29 (19–43)	.004[c]	19 (16–22)
Replication cohort (DIMS2)				
N	15	8		8
Male gender, %	67	50	.66[a]	50
Mean age, y (SD)	40.5 (13.0)	48.8 (18.0)	.22[b]	60.2 (8.9)
Medication, n (%)				
Topical steroids	13 (87)	5 (63)	.30[a]	
Periocular steroids <3 months	4 (27)	1 (13)	.62[a]	
Systemic steroids	1 (7)	2 (25)	.27[a]	
DMARDS or biologicals	2 (13)	0	.53[a]	
Anterior chamber cell count, n (%)[d]				
0	2 (14)	3 (38)		NA
0.5+	5 (36)	1 (13)		NA
1+	2 (14)	1 (13)		NA
2+	2 (14)	3 (38)		NA
3+	2 (14)	0		NA
4+	1 (7)	0		NA
Hypopyon	0	0		NA
Mean storage time, months (range)	64 (12–116)	26 (18–37)	.001[c]	22 (19–24)
Discovery cohort (LC-MS/MS)				
N	9	5		5
Male gender, %	67	0	.03[a]	0
Mean age, y (SD)	35.2 (11.6)	55.7 (14.7)	.01[b]	60.7 (7.7)
Medication, n (%)				
Topical steroids	8 (89)	4 (80)	1.00[a]	
Periocular steroids <3 months	2 (22)	1 (20)	1.00[a]	
Systemic steroids	1 (11)	1 (20)	1.00[a]	
DMARDS or biologicals	1 (11)	0	1.00[a]	
Anterior chamber cell count, n (%)				
0	0	2 (40)		NA
0.5+	2 (22)	1 (20)		NA
1+	2 (22)	1 (20)		NA
2+	4 (44)	1 (20)		NA

Continued on next page

TABLE 1. Study cohorts (*Continued*)

	B27-AAU	Idiopathic AAU	*P* Value	CAT
3+	1 (11)	0		NA
4+	0	0		NA
Hypopyon	0	0		NA
Mean storage time, months (range)	84 (43–137)	54 (42–67)	.053[c]	42 (40–43)

B27-AAU = human leukocyte antigent-B27–associated acute anterior uveitis; CAT = cataract; DIMS = direct infusion mass spectrometry; DMARDS = disease-modifying antirheumatic drugs; LC-MS/MS = liquid chromatography/tandem mass spectrometry; NA = not applicable; SD = standard deviation.

[a]Fisher exact test.

[b]*t* test.

[c]Mann-Whitney *U* test.

[d]Anterior chamber cell count was unavailable from 1 patient in the B27-AAU group.

To shed more light on the role of HLA-B27 in disease, we investigated metabolic profiles of B27-AAU and idiopathic AAU patients as close to the site of inflammation as possible: the aqueous humor (AqH). To aid in the identification of metabolites, we combined 2 rounds of untargeted metabolomics via direct infusion mass spectrometry (DIMS) to comprehensively map the metabolic patterns of AqH. Using unsupervised and supervised exploratory data mining, we prioritized a set of features for validation by (semi-) targeted liquid chromatography/tandem mass spectrometry (LC-MS/MS).[13,14]

METHODS

• **PATIENTS AND PATIENT MATERIAL:** This cross-sectional case-control study was approved by the Medical Ethical Committee of the University Medical Center Utrecht. All patients signed informed consent. The demographic characteristics of the cohorts are shown in Table 1. In total, 70 samples were analyzed using DIMS technology (see below) in 2 independent cohorts. AqH samples from 30 patients with B27-AAU, 18 patients with idiopathic AAU, and 22 patients with cataracts (CATs) were collected between 2006 and 2014 and randomly assigned to either a discovery (n = 39) or replication cohort (n = 31). Idiopathic AAU was defined as HLA-B27–negative (determined by HLA typing) noninfectious AAU without clinical evidence for an uveitis-associated systemic condition (eg, rheumatic conditions). All uveitis patients underwent a full ophthalmologic examination by an experienced ophthalmologist as well as routine laboratory screening and radiography of the lungs. Laboratory screening included erythrocyte sedimentation rate and screening for various infectious agents in serum, including syphilis, Lyme disease, and an interferon-gamma release assay tuberculosis test. In all patients with idiopathic AAU the AqH was tested for herpes simplex virus and varicella zoster virus by polymerase chain reaction study and Goldmann-Witmer coefficients. Specimens used for analysis were either the remainders from samples taken for diagnostic purpose to rule out an infectious cause or were obtained during ocular surgery for disease complications (eg, CAT or glaucoma surgery; B27-AAU n = 3, IAU n = 1). AqH from patients with CAT with no history of ocular inflammatory disease was obtained during CAT surgery. All AqH samples (±20-75 μL) were stored at –80°C directly after sampling.

• **DIMS ANALYSIS:** A diagram of the workflow used to establish metabolic profiles is shown in Figure 1. Per sample, a volume of 20 μL was mixed with 20 μL 0.6% formic acid in Milli-Q ultrapure water (Merck, Darmstadt, Germany) and 93.3 μL Amino Acid and Carnitine/Acylcarnitine Tuning Standards (set NSK-AB) according to manufacturer's instructions (Cambridge Isotope Laboratories, Tewksbury, MA, USA). After filtration over a 0.2-μm cutoff filter plate, the sample was analyzed by DIMS using an Advion TriVersa NanoMate (Ithaca, NY, USA) with 5-μm ID chip-based infusion and a Q-Exactive Plus mass spectrometer (Thermo Scientific, Bremen, Germany). Mass spectrometry data were acquired in the scan range of 70-600 m/z. The system was operated at a resolution of 140,000 in both positive and negative mode (1.5 min each at 1.6 kV). To achieve high mass accuracy, mass calibration was performed before each experiment and internal lock masses were used. The mean intensity of 3 technical replicates was used for downstream computational analysis. For downstream analysis we only considered the negative electrospray ionization mode of the acquired dataset, because the ocular fluid samples were stored in polyethylene glycol containing Eppendorf tubes, which suppressed signals for other metabolites in the positive mode. Raw data files were converted to mzXML format using MSConvert and processed using an in-house–developed untargeted metabolomics pipeline as described previously as well as the Human Metabolome Database (accurate mass, isotopic pattern).[15]

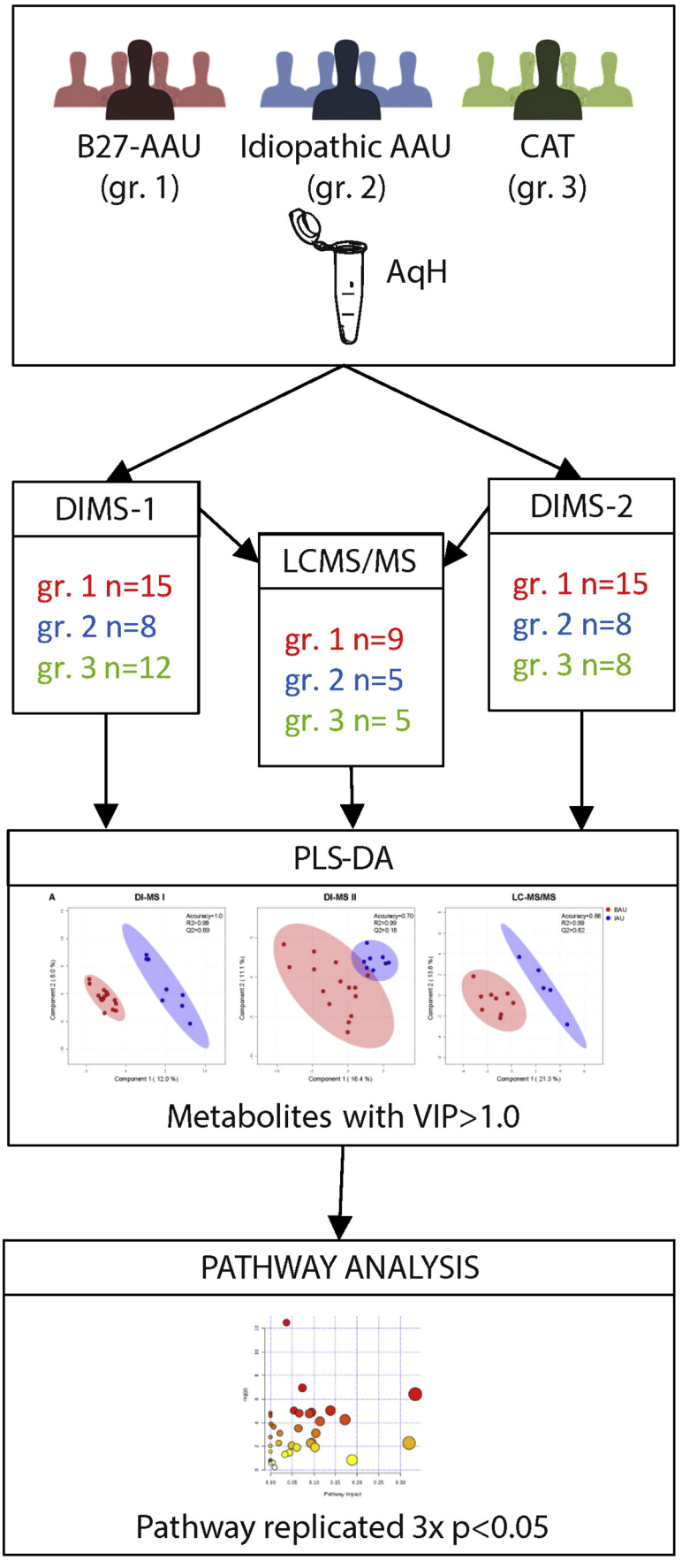
B27-AAU
(gr. 1)
Idiopathic AAU
(gr. 2)
CAT
(gr. 3)
AqH
DIMS-1
gr. 1 n=15
gr. 2 n=8
gr. 3 n=12
LCMS/MS
gr. 1 n=9
gr. 2 n=5
gr. 3 n= 5
DIMS-2
gr. 1 n=15
gr. 2 n=8
gr. 3 n=8
PLS-DA
A
DI-MS I
DI-MS II
LC-MS/MS
Metabolites with VIP>1.0
PATHWAY ANALYSIS
Pathway replicated 3x p<0.05

• **LC-MS/MS ANALYSIS:** To validate the metabolites of interest identified by DIMS, we performed LC-MS/MS in triplicate (technical replicates) on AqH samples with sufficient volume left after DIMS (n = 19). To prepare the samples for LC-MS analysis, we let 100-μL internal standards mixture in methanol evaporate to dryness in an Eppendorf vial, after which we added 50 μL of (cold) sample to the residue together with 10 μL 4 M ice cold perchloric acid. After vortex mixing, the mixture was put on ice for 5 minutes and the vial was centrifuged at 13,000 *g* at 4°C and 48 μL was accurately transferred to a new vial. A volume of 2 μL 2 M potassium hydroxide was added to neutralize the sample and precipitate the excess of perchloric acid. After keeping on ice for 5 minutes after vortex mixing, the sample was centrifuged at 13,000 *g* for 5 minutes at 4°C. The supernatant was transferred to a clean glass vial for LC-MS analysis. Analysis was performed using a Phenomenex Luna Omega PS C18 column (2.1 × 100 mm, 1.6 μm) positioned in an Acella ultra-high-performance liquid chromatography system operated at 30° and a flow rate of 150 μL per minute^{-1}. Upon sample injection, a period of 3-minute 100% solution A (6.5 mM ammoniumbicarbonate pH8) was followed by a 2.5-minute linear gradient to 10% B (95% methanol plus 5% 6.5 mM ammoniumbicarbonate pH8). After this, the concentration B was linearly increased to 98% in 4.4 minutes and kept there for 4 minutes. Finally, the column was reconditioned at 100% A for 4 minutes before the next injection. An LTQ-Orbitrap XL was used for MS detection. Mass calibration was performed before analysis. The system was operated in data-dependent analysis MS/MS mode at a resolution of 30,000 in negative mode at a potential of 3.5 kV and a capillary temperature of 300°C. Peak identifications were performed in a search against the Human Metabolome Database (accurate mass and isotopic pattern) and a custom database (retention time, m/z, and fragmentation pattern).

• **DATA PROCESSING AND STATISTICAL ANALYSIS:** High-quality peaks and putative metabolites that were detected in the majority of samples (the relative standard deviations of peak intensities and retention time were evaluated) were loaded into the Metaboanalyst 3.0 server. To improve data quality, samples with a high percentage of missing values were identified and removed; data from the DIMS analyses were filtered by interquartile range of intensity and were considered if they were detected in >70% of all samples. Data normalization was achieved by quantile normalization and autoscaling of the dataset (plus log-transformation of the LC-MS/MS data to achieve normal distribution). We used exploratory data analysis, including principal component analysis, partial least square-discriminant analysis (PLS-DA), and hierarchical clustering with Euclidean distance and the Ward clustering method.[16,17] Based upon principal component analysis, we excluded 4 samples from the discovery cohort with strongly deviating coefficients for the first 2 components (idiopathic AAU n = 2, CAT n = 2) (Supplemental Figure 1; Supplemental Material available at AJO.com). The observation that these 4 outliers show a relatively similar distance from the other samples on Principal Component 1 (PC1) suggests technical error over clinical variation. Therefore, these 4 samples were not considered for additional analysis.

A variable importance in projection (VIP) score was obtained from the PLS-DA analysis for each metabolite. A variable with a VIP score >1 can be considered important in driving the projection used to summarize the PLS-DA model in which the groups are optimally separated.

The predicted metabolites with a VIP score >1 were fed into the integrated pathway analysis module of the MetaboAnalyst server 3.0. Metabolic pathways were considered affected if metabolites functioning in their enzymatic reactions were found in altered abundance (replicated at $P <$ .05) across all 3 individual runs (DIMS1 plus DIMS2 plus LCMS). A Mann-Whitney *U* test (SPSS software version 21; SPSS, Inc., Chicago, IL, USA) was used to determine group differences between idiopathic AAU and B27-AAU and the direction of effect of individual metabolites derived from the pathway analysis.

Individual metabolites were tested for correlation with age or uveitis activity (anterior chamber cell count according to the standardization of uveitis nomenclature recommendations[18]) using the Spearman ρ test. Metabolite abundance between male and female patients was tested using a Mann-Whitney *U* test. Metabolites were influenced by age, sex, or uveitis activity if a significant effect in the same direction was found in all 3 runs. In addition, Z score transformed data of all 3 runs were accumulated (Z = variable–mean$_{group}$/standard deviation$_{group}$) for combined analysis. CAT samples were used for reference only and were not taken into consideration for statistical testing.

FIGURE 1. Flow diagram of methods used to identify meaningful metabolic differences between human leukocyte antigent-B27–associated acute anterior uveitis (B27-AAU) and idiopathic AAU. Patients with noninflammatory cataracts (CAT) were used as a reference but were not taken into consideration for partial least square-discriminant analysis (PLS-DA) modeling. Aqueous humor (AqH) from patients and control subjects (top panel) was analyzed with direct infusion mass spectrometry (DIMS) in 2 independent cohorts (second panel). Relevant identified metabolites were validated by liquid chromatography/tandem mass spectrometry (LC-MS/MS). Metabolic profiles were analyzed by PLS-DA for all 3 runs (DIMS1, DIMs-2, and LC-MS/MS; third panel). Metabolites with a variable influence in the projection (VIP) score of > 1.0 in this model were then entered into pathway enrichment analysis for each run (Metabolanalyst 3.0) (bottom panel). Pathways that were significantly indicated and replicated in all runs were considered to be significantly involved in AAU.

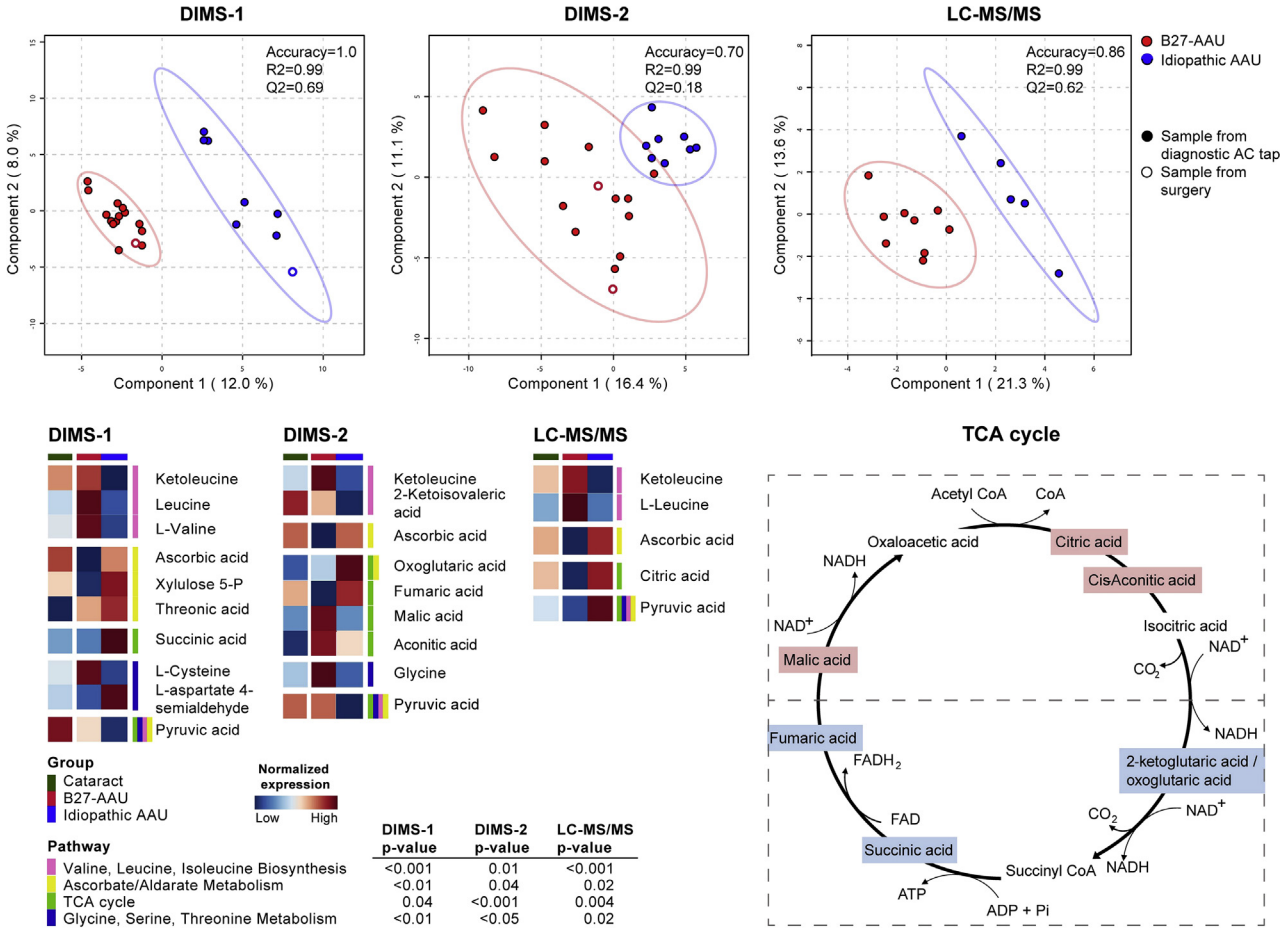

FIGURE 2. The metabolic composition of aqueous humor in patients with human leukocyte antigent-B27–associated acute anterior uveitis (B27-AAU) is distinct from idiopathic AAU. Top panel: Partial least square-discriminant analysis (PLS-DA) of the intraocular metabolome separates B27-AAU (red) from idiopathic AAU (blue) in all 3 runs, indicating metabolic heterogeneity between these AAU entities. Filled dots represent leftover samples from diagnostic anterior chamber (AC) tap, while open circles represent samples taken during intraocular surgery. The explained variance of each component is shown in brackets. Ellipses display 95% confidence intervals for the samples of the group. Accuracy values from internal cross-validation are given in the right corner of the graphs: R2 = fraction of y-variation modeled in the component (goodness of fit), Q2 = overall cross-validated R2 for the component (predictive ability). Bottom left: Replicated metabolic pathways in colors that were different between B27-AAU and idiopathic AAU in aqueous humor. Pathways are based on metabolites that had a variable influence in the projection score of > 1.0 in the PLS-DA (Table 3). For each metabolite, the mean peak intensity for direct infusion mass spectrometry (DIMS) and retention time for liquid chromatography/tandem mass spectrometry (LC-MS/MS) are shown for patients with B27-AAU, idiopathic AAU, and cataracts (CAT, green) as a reference. Bottom right: Metabolites in the tricarboxylic acid (TCA) cycle that are significantly decreased or increased in the aqueous humor of patients with B27-AAU compared with patients with idiopathic AAU in ≥1 run. Blue: Decreased in patients with B27-AAU versus patients with idiopathic AAU. Red: Increased in patients with B27-AAU versus patients with idiopathic AAU.

RESULTS

• **B27-AAU AND IDIOPATHIC AAU SHOW DIFFERENCES IN METABOLIC AQH PROFILES:** Metabolic profiling was performed in 3 rounds using different cohorts of patients (Figure 1). The demographic characteristics of each cohort are shown in Table 1. Age and sex were similar between the groups in DIMS1 and DIMS2 analyzed by DIMS but not for the LC-MS/MS cohort (Table 1). The mean storage time of the AqH samples of the B27-AAU was longer compared with samples from the idiopathic AAU group. The treatment regimens did not vary between the 2 uveitis groups. In both cohorts there were some patients with a (related) systemic disease in the B27-AAU group: in the first cohort (DIMS1) there were 2 of 15 (13%) patients with AS and 1 patient with psoriasis in the B27-AAU group. In DIMS2 there were 4 of 15 (27%) patients with AS in the B27-AAU group. These patients harbored a relatively similar

TABLE 2. The 20 Replicated Metabolites Identified Across All 3 Mass Spectrometry Runs in the Aqueous Humor of Patients With Acute Anterior Uveitis

Putative metabolite	and/or	N	*P* Value	VIP	Ratio[a]	N	*P* Value	VIP	Ratio[a]	N	*P* Value	VIP	Ratio[a]
			DIMS1				DIMS2				LC-MS/MS		
Ascorbic acid		23	.12	1.60[b]	0.44	23	.004[b]	1.82[b]	0.15	12	.04[b]	1.46[b]	0.39
Butyric acid (butanoic acid)		23	.08	0.92	1.52	23	.48	0.89	0.48	9	.12	1.13[b]	0.65
Citric acid	Isocitric acid	23	1.00	0.26	1.27	23	.05[b]	0.96	0.67	14	.10	1.45[b]	0.79
Fumaric acid	Maleic acid	23	.25	0.55	0.67	23	.03[b]	1.26[b]	0.55	9	.04[b]	0.56	0.42
Glutamine		23	.65	0.85	1.06	23	.02[b]	0.71	0.74	14	.13	0.96	5.85
Hexanoic acid (caproic acid)		23	.002[b]	2.09[b]	2.32	23	.25	0.86	0.38	11	.19	0.61	0.79
Hippuric acid		23	.65	0.84	0.94	23	.65	0.91	1.05	13	.56	0.50	1.72
Indole		23	.001[b]	1.74[b]	1.61	23	.95	1.24[b]	0.96	14	.84	0.64	0.58
Ketoleucine (4-methyl-2-oxopentanoate)	3-methyl-2-oxopentanoate	23	.09	1.30[b]	1.23	23	.22	1.23[b]	1.11	14	.006[b]	1.54[b]	4.66
Leucine	Isoleucine	23	.09	1.34[b]	1.54	—	—	—	—	14	.02[b]	1.23[b]	5.39
Phenylalanine		23	.11	0.33	0.60	23	1.00	1.11[b]	1.02	14	.95	0.51	0.95
Phenylpyruvic acid		23	.12	0.40	1.08	23	.40	0.85	0.96	14	.32	0.87	1.33
Pivalic acid	(Iso-) valeric acid	23	.006[b]	0.95	1.55	23	.25	0.80	0.41	13	.24	0.99	0.56
Pyruvic acid		23	.05	1.12[b]	3.15	23	.20	1.30[b]	1.37	14	.16	1.54[b]	0.70
Succinic acid (butanedioic acid)	Methylmalonic acid	23	.004[b]	1.31[b]	0.41	23	.12	0.95	0.79	10	.73	0.61	0.59
Threonic acid	Erythronic acid	23	.05	1.26[b]	0.49	23	.16	0.83	0.67	14	.55	0.79	0.86
Tryptophan		23	.18	0.71	0.91	23	.27	0.42	0.67	14	.84	1.14[b]	0.98
Tyrosine		23	.37	1.42[b]	0.83	23	.44	0.32	0.95	14	.39	0.74	1.76
Uric acid		23	.01[b]	1.04[b]	2.11	23	.85	1.35[b]	1.12	14	.05	1.66[b]	1.49

DIMS = direct infusion mass spectrometry; LC-MS/MS = liquid chromatography/tandem mass spectrometry; PLS-DA = partial least square-discriminant analysis; VIP = variable importance in projection.

Note: From the PLS-DA analysis the VIP score was obtained for each metabolite. A variable with a VIP score >1 can be considered important in driving the projection used to summarize the PLS-DA model in which the groups are optimally separated.

[a]Ratio of patients with B27-AAU/patients with idiopathic AAU.

[b]Significant *P* values (<.05, Mann Whitney *U* test between patients with B27-AAU and patients with idiopathic AAU) or VIP scores >1.0.

AqH metabolic profile compared with the other B27-AAU patients (Supplemental Figure 2; Supplemental Material available at AJO.com).

We performed 2 rounds of metabolic profiling of AqH of B27-AAU, idiopathic AAU, and CAT patients using DIMS, which resulted in the identification of 147 metabolic compounds in the discovery cohort and 127 in the replication cohort (Supplemental Table 1; Supplemental Material available at AJO.com). Direct comparison of the metabolic profiles by principal component analysis revealed no consistent separate clusters for any of the groups that most likely can be attributed to the relatively large within-group variation (compared with between-group variation) (Supplemental Figure 2; Supplemental Material available at AJO.com). To reveal more sophisticated differences between the 2 disease groups, we exploited supervised dimensionality reduction by discriminant analysis via PLS-DA. PLS-DA generated excellent separation by low-dimensional projection of the disease groups with sufficient predictive accuracy for both DIMS runs as determined by internal cross validation of the projected models (Figure 2, top). The metabolites considered to drive these differences (VIP score >1.0 of the PLS-DA) were mostly short-chain fatty acids and branched-chain amino acids (BCAAs). Therefore, we subjected samples with sufficient volume left after DIMS to LC-MS/MS with standard compounds for (semi-)targeted validation directed at small fatty acids and organic acids. LC-MS/MS analysis yielded 29 metabolites that were detected in >70% of all patients (Supplemental Table 1; Supplemental Material available at AJO.com). In total, 18 annotated metabolites were considered detected in all 3 runs (DIMS1, DIMS2, and LC-MS/MS), and leucine in 2 of 3 runs (LC-MS/MS and the first DIMS) (Table 2). We compared the intensity levels of DIMS and LC-MS/MS for each of these 19 metabolites measured in the same samples, which demonstrated a positive correlation between DIMS and LC-MS/MS intensities for 6 metabolites (Supplemental Figure 3; Supplemental Material available at AJO.com). Finally, of these 6 robustly identified metabolites, 2 also showed a VIP score >1.0 in all 3 runs: ketoleucine and uric acid. Ascorbic acid and pyruvic acid also had a VIP score >1.0 in all 3 runs (Table 2), but

TABLE 3. Pathway Enrichment Analysis Based on Metabolites Identified by Partial Least Square-Discriminant Analysis for Each Mass Spectrometry Run

Mass Spectrometry Run	Pathway Name	Hits	*P* Value	Impact	Details
	Phenylalanine, tyrosine, and tryptophan biosynthesis[a]	6/27	<.001	0.04	Indoleglycerol phosphate, indole, L-tyrosine, 6-deoxy-5-ketofructose 1-phosphate, L-aspartate-semialdehyde, 4-hydroxyphenylpyruvic acid
DIMS-1	Valine, leucine, and isoleucine biosynthesis[b]	4/27	<.001	0.07	Pyruvic acid, L-leucine, L-valine, ketoleucine
	Arginine and proline metabolism[a]	6/77	.002	0.33	Ornithine, L-proline, hydroxyproline, creatine, urea-1-carboxylate, pyruvic acid
	Phenylalanine metabolism[a]	4/45	<.01	0.05	Phenylacetic acid, pyruvic acid, succinic acid, L-tyrosine
	Ascorbate and aldarate metabolism[b]	4/45	<.01	0.14	Ascorbid acid, pyruvic acid, threonic acid, xylulose 5-phosphate
	Lysine degradation	4/47	<.01	0.09	Trimethyl-L-lysine, glutaric acid, oxoadipic acid, carnitine
	Aminoacyl-tRNA biosynthesis	5/75	<.01	0.00	L-cysteine, L-valine, L-leucine, L-tyrosine, L-proline
	Glycine, serine, and threonine metabolism[b]	4/48	<.01	0.07	L-aspartate-semialdehyde, creatine, L-cysteine, pyruvic acid
	Tyrosine metabolism	5/76	<.01	0.09	L-thyrosine, 4-hydroxyphenylpyruvic acid, vanillylmandelic acid, pyruvic acid, succinic acid
	Pantothenate and coenzyme A biosynthesis[a]	3/27	.01	0.00	L-cysteine, L-valine, pyruvic acid
	Cysteine and methionine metabolism	4/56	.01	0.17	L-cysteine, L-cystine, pyruvic acid, L-aspartate-semialdehyde
	Pentose phosphate pathway	3/32	.02	0.11	Gluconic acid, xylulose 5-phosphate, pyruvic acid
	Propanoate metabolism	3/35	.02	0.00	Succinic acid, L-lactic acid, L-valine
	Glutathione metabolism	3/38	.03	0.01	L-cysteine, ornithine, ascorbic acid
	Valine, leucine, and isoleucine degradation[a]	3/40	.03	0.06	L-leucine, L-valine, ketoleucine
	Citrate cycle (TCA cycle)[b]	2/20	.04	0.10	Succinic acid, pyruvic acid
	Taurine and hypotaurine metabolism	2/20	.04	0.02	Pyruvic acid, L-cysteine
DIMS-2	Citrate cycle (TCA cycle)[b]	5/20	<.001	0.29	Oxoglutaric acid, L-malic acid, aconitic acid, pyruvic acid, fumaric acid
	Phenylalanine, tyrosine, and tryptophan biosynthesis[a]	5/27	<.001	0.26	Shikimic acid, indole, L-phenylalalnine, 3-dehydroquinate, 2-aminobenzoic acid
	Alanine, aspartate, and glutamate metabolism	4/24	<.001	0.00	N-acetyl-L-aspartic acid, pyruvic acid, oxoglutaric acid, fumaric acid
	Pantothenate and coenzyme A biosynthesis	4/27	<.001	0.25	Pantothenic acid, alpha-ketoisovaleric acid, pyruvic acid, uracil
	Butanoate metabolism[a]	4/40	<.01	0.13	4-hydroxybutyric acid, pyruvic acid, oxoglutaric acid, fumaric acid
	Glyoxylate and dicarboxylate metabolism[a]	4/50	<.01	0.03	Aconitic acid, oxoglutaric acid, L-malic acid, pyruvic acid
	Valine, leucine, and isoleucine biosynthesis[b]	3/27	.01	0.14	Pyruvic acid, alpha-ketoisovaleric acid, ketoleucine
	β-Alanine metabolism	3/28	.01	0.01	Malonic acid, pantothenic acid, uracil
	Vitamin B6 metabolism	3/32	.02	0.12	Oxoglutaric acid, pyridoxal, pyruvic acid
	Nitrogen metabolism	3/39	.03	0.00	L-phenylalalnine, 2-aminobenzoic acid, glycine
	Nicotinate and nicotinamide metabolism	3/44	.04	0.00	Pyruvic acid, porpionic acid, fumaric acid
	Phenylalanine metabolism[a]	3/45	.04	0.12	L-phenylalalnine, pyruvic acid, fumaric acid
	Ascorbate and aldarate metabolism[b]	3/45	.04	0.13	Ascorbic acid, pyrvic acid, oxoglutaric acid
	Arginine and proline metabolism[a]	4/77	.04	0.13	Proline, creatine, fumaric acid, pyruvic acid
	Tryptophan metabolism	4/79	.04	0.19	Indole, aminobenzoic acid, 3-hydroxyanthranilic acid, indoleacetic acid

Continued on next page

TABLE 3. Pathway Enrichment Analysis Based on Metabolites Identified by Partial Least Square-Discriminant Analysis for Each Mass Spectrometry Run (*Continued*)

Mass Spectrometry Run	Pathway Name	Hits	*P* Value	Impact	Details
LC-MS/MS	Glycine, serine, and threonine metabolism[b]	3/48	<.05	0.19	Glycine, creatine, pyruvic acid
	Valine, leucine, and isoleucine biosynthesis[b]	3/27	<.001	0.06	Pyruvic acid, L-leucine, ketoleucine
	Butanoate metabolism[a]	3/40	<.001	0.09	Pyruvic acid, butyric acid, diacetyl
	Citrate cycle (TCA cycle)[b]	2/20	.004	0.15	Citric acid, pyruvic acid
	Valine, leucine, and isoleucine degradation[a]	2/40	.02	0.06	L-leucine, ketoleucine
	Ascorbate and aldarate metabolism[b]	2/45	.02	0.13	Ascorbate, pyruvic acid
	Glycine, serine, and threonine metabolism[b]	2/48	.02	0.00	Pyruvic acid, L-tryptophan
	Glyoxylate and dicarboxylate metabolism[a]	2/50	.02	0.00	Citric acid, pyruvic acid

DIMS = direct infusion mass spectrometry, LC-MS/MS = liquid chromatography/tandem mass spectrometry, TCA = tricarboxylic acid.

Note: Metabolites identified by partial least square-discriminant analysis with a variable importance in projection score >1.0 were analyzed by the Integrated Pathway Analysis Module of the MetaboAnalyst server 3.0 that resulted in the pathways shown in Table 3. The hits indicate the number of metabolites identified for each metabolic pathway (the number of metabolites found in this study/the number of metabolites known to be involved in the pathway). The impact score is a combination of the centrality of the metabolites within a certain pathway and pathway enrichment results and ranges from 0-1. The putative metabolites from DIMS or LC-MS/MS analyses that represent the "hits" for the pathway they are in are listed in the Details column.

[a]Pathway present in 2 of 3 analyses.

[b]Pathway present in all 3 analyses.

these (putative) metabolites did not correlate between DIMS and LC-MS/MS ($\rho = 0.15$, $P = .58$ and $\rho = -0.10$, $P = .69$, respectively).

• **AQH FROM B27-AAU PATIENTS CHARACTERIZED BY HIGHER VALINE/LEUCINE BIOSYNTHESIS, LOWERED ASCORBATE METABOLISM, AND CHANGES IN ENERGY METABOLISM:** Next, we considered all metabolites with a VIP score >1.0 from each individual run (n = 53 for DIMS1, n = 52 for DIMS2, and n = 12 for LC-MS/MS) and subjected them to metabolic pathway analysis, with the aim to identify involved metabolic pathways consistently detected across all 3 runs. We detected 4 pathways in all cohorts; the BCAA or valine, leucine, and isoleucine biosynthesis (Kyoto Encyclopedia of Genes and Genomes [KEGG] ko00290, increased in B27-AAU), the ascorbate and aldarate metabolism pathway (KEGG ko00053, decreased in B27-AAU), the citric acid cycle (also known as the tricarboxylic acid [TCA] cycle or Krebs cycle, KEGG ko00020), and the glycine, serine, and threonine metabolism pathway (KEGG ko00260) (Table 3). The relative abundance of the key metabolites of these pathways identified in B27-AAU and idiopathic AAU are shown in Figure 2 (bottom).

• **DISCOVERY, REPLICATION, AND VALIDATION OF KETOLEUCINE AS A POTENTIAL MOLECULAR MARKER FOR DISEASE ACTIVITY IN ANTERIOR UVEITIS:** We tested the individual metabolites that were replicated (ascorbic acid and ketoleucine) for an association with disease activity (anterior chamber cell count), age, sex, treatment, and storage time. We observed no correlation between any of these characteristics and ascorbic acid or ketoleucine (see Supplemental Figure 4 for details on ketoleucine and storage time; Supplemental Material available at AJO.com) besides disease activity: a negative correlation with disease activity was evident for ascorbic acid, for data obtained by DIMS1 ($\rho = -0.46$, $P = .03$), with evidence for a similar trend in the other 2 runs ($\rho = -0.35$, $P = .11$ and $\rho = -0.32$, $P = .31$ for DIMS2 and LC-MS/MS, respectively). Ketoleucine correlated positively ($\rho = 0.41$–0.81) with anterior chamber cell count—a hallmark sign of disease activity in AAU—in all 3 runs (Figure 3). This was most striking for the standard compound controlled LC-MS/MS ($\rho = 0.81$, $P < .001$) and mainly driven by patients with B27-AAU (Figure 3, right).

DISCUSSION

USING MULTIPLE DETECTION PLATFORMS AND INDEPENDENT patient cohorts, we aimed to characterize the metabolic profile of AqH of patients with B27-AAU and (noninfectious) idiopathic AAU and observed that these clinically analogous conditions are accompanied by unique differences in metabolic profiles. These changes included metabolites present in BCAA metabolism, ascorbate and aldarate metabolism, the TCA cycle, and serine biosynthesis. Previous metabolic profiling of plasma of patients with AAU showed mainly involvement of amino acid, carbohydrate, and lipid metabolism, and in part reflect our observations in AqH.[11]

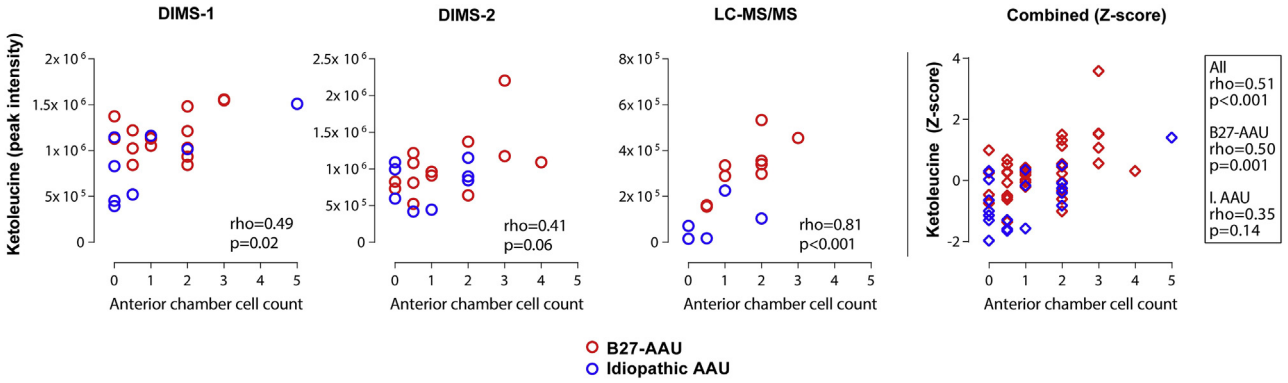

FIGURE 3. Ketoleucine correlates with anterior chamber cell count in acute anterior uveitis (AAU). The peak intensity of ketoleucine for direct infusion mass spectrometry 1 (DIMS1), direct infusion mass spectrometry 2 (DIMS2), and liquid chromatography/tandem mass spectrometry (LC-MS/MS) or the normalized (Z) score of all 3 runs combined is indicated on the y axis. On the x axis is the anterior chamber cell count shown according to the standardization of uveitis nomenclature recommendations (scale 0-4+). A score of 5 represents hypopyon. Dots represent original data (peak intensities), diamonds represent normalized (Z score) data. Red: Patients with human leukocyte antigent-B27–associated acute anterior uveitis (B27-AAU). Blue: Patients with idiopathic AAU.

In our study, several metabolites from the BCAA biosynthesis pathway were increased in B27-AAU, indicating a role for the BCAA biosynthesis pathway in B27-AAU over idiopathic AAU. Among the intermediates of this pathway, ketoleucine (a deaminated derivate of leucine) scored a VIP >1.0 in PLS-DA analysis of all 3 MS runs and showed good correlation between DIMS and LC-MS intensities. Ketoleucine (also known as 4-methyl-2-oxopentanoate, α-ketoisocaproic acid, or 2-ketoisocaproate) is interconverted from leucine by BCAA transaminase (BCAT1) and BCAT2 as the first step in BCAA catabolism.[19] Interestingly, selective blocking of the BCAT1 activity in macrophages—a cell type considered central to initiating endotoxin-induced uveitis in rodents[20,21]—results in a dramatic attenuation of disease activity in inflammatory mouse models (eg, collagen-induced arthritis) by redirecting the inflammatory macrophage transcriptome to a regulatory phenotype (so-called M2 cells).[22]

About half of patients with B27-AAU will eventually develop AS, a rheumatic condition that shares a risk factor for disease development in HLA-B27 and is intimately linked to (subclinical) intestinal inflammation and gut microbiome dysbiosis.[23,24] BCAA levels are also changed in the plasma/serum of patients with AS.[25,26] Importantly, there are indications that the microbiome might be dependent on the HLA haplotype[27]; more specifically, HLA-B27 transgenic rats showed gut dysbiosis.[28] Interestingly, the gut microbiome contributes to altered levels of BCAAs[29] and fecal matter of patients with ASs show changes in the BCAAs valine, leucine, and ketoleucine that correlate with erythrocyte sedimentation rate—a clinical sign of inflammation.[30] It should be noted that the alterations in BCAA levels found in gut or serum of patients with AS were not observed in patients with rheumatoid arthritis and are in line with our observations that BCAA metabolism may be specifically affected in HLA-B27–linked pathology. Although ketoleucine is also known for its neurotoxic properties, the size of our cohorts and retrospective nature did not allow for satisfactory testing of optic nerve involvement. We did, however, observe 2 patients with B27-AAU (1 in each cohort) with optic disc swelling at the time of sampling.

Ketoleucine can be released from the cell but is commonly reaminated into leucine. Leucine has been shown to be a potent activator of the proinflammatory mammalian target of rapamycin signaling pathway, and inhibiting mammalian target of rapamycin is shown to be effective in treating noninfectious uveitis.[31–34] Alternatively, ketoleucine can be decarboxylated into downstream intermediates (eg, acetyl-CoA) that fuel other metabolic pathways, such as the TCA cycle. The involvement of the TCA cycle was evident from increase in malic, citric, and aconitic acids in B27-AAU compared with idiopathic AAU, while subsequent intermediates derived from aconitic acid (2-ketogultaric acid, succinic acid, and fumaric acid) were lower in B27-AAU compared with idiopathic AAU, forming a "break" between aconitic acid and 2-ketoglutaric acid (Figure 2). Curiously, a similar fragmentation of the TCA cycle is a hallmark of the metabolic shift from resting (M0) to proinflammatory (M1) macrophages.[35,36] The local cell subset(s) driving this "TCA-signature" of B27-AAU provide an exciting field of upcoming research.

Ascorbate and aldarate metabolism was decreased in B27-AAU compared with idiopathic AAU. Ascorbate (or ascorbic acid, also known as vitamin C) protects from inflammatory damage and attenuates inflammation as an antioxidant as well as through the inhibition of nuclear factor-κB signaling.[37,38] Intraocular ascorbate levels are known to

decrease in the endotoxin-induced uveitis models of AAU described above.[39]

Collectively, these findings point toward more inflammatory activity in B27-AAU compared with idiopathic AAU, which raises the question whether the metabolic differences detected reflect distinct pathology or merely differences in disease activity (or the resulting increased amount of infiltrating cells in the anterior chamber) between the 2 conditions. Indeed, we did observe a positive correlation between ketoleucine and anterior chamber cell count (and perhaps an inverse relation between ascorbate and anterior chamber cell count exists as well). However, the correlation between ketoleucine and disease activity was predominantly observed in B27-AAU and—considering the BCAA link with AS—differences in this BCAA derivate may well be related to HLA-B27 pathology and disease activity. Although treatment may influence metabolism (and disease activity), the treatment regimens did not differ between B27-AAU and idiopathic AAU (Table 1), therefore, we consider the effect of therapy on the study results to be minimal.

The metabolites identified in this study are most likely the product of surrounding tissue or (apoptotic) infiltrating cells. Because apoptotic cells and cell debris (ie, hypopyon) are features of AAU, we deliberately did not spin down the AqH samples before storage to capture the full metabolic spectrum within the anterior chamber. Future studies are needed to identify the source and cell type responsible for the observed metabolic differences. However, apoptotic cell death can be regulated by engagement of the cell death surface receptor Fas by Fas ligand (FasL). As FasL is elevated in AqH of AAU and most of the cellular infiltrate in human AAU is Fas-positive, a proapoptotic (or necrotic) environment for infiltrated cells in AqH is facilitated.[40] HLA-B27 AAU may show a typical polymorphonuclear cell pattern on optical coherence tomography of the anterior chamber.[41] Also, lipopolysaccharide-induced anterior ocular inflammation is accompanied by a strong influx of granulocytes that express the apoptosis mediator caspase-3.[42] Considering this, we expect substantial "leakage" of cellular metabolic products from infiltrating and surrounding tissues during inflammation of the anterior chamber. In support of this is the correlation of ketoleucine with anterior chamber cell count. However, because this correlation seemed limited to HLA-B27 AAU, it is tempting to speculate that either a different cellular composition or metabolic programming may lead to the higher ketoleucine levels in B27-AAU.

Regardless, the activity of the inflammation in the anterior segment significantly guides clinical decision making in patients with AAU. Objective quantification of this process has therefore been a key research goal for years in ophthalmology. To overcome interobserver variability of manual counting of infiltrating cells (anterior chamber cell counting) by ophthalmologists, anterior segment optical coherence tomography and laser flare photometry have been developed as more objective imaging methods to assess disease activity.[43,44] We provide the rationale that evaluation of metabolic markers could complement monitoring disease activity in patients with B27-AAU.

Emerging metabolomics studies of eye disease demonstrate its clinical potential. For example, metabolomics signatures have been shown to predict diabetic retinopathy[45] or the formation of CAT.[46] Also, the distinct metabolic makeup across stages of age-related macular degeneration[47] suggests rewiring of ocular metabolism, and reprogramming these metabolic pathways has been suggested as a way to rescue retinal degeneration.[48] Metabolomics can also be used to find early biomarkers for ocular diseases, such as glaucoma, or for in-depth evaluation of pharmacokinetics in AqH.[49,50] Our results in AAU pave the way for metabolomics studies in the clinical management of uveitis. For example, we envision that elucidating the Raman signatures of BCAAs, such as ketoleucine, may catalyze the development of noninvasive monitoring of these metabolites in the anterior chamber using Raman spectroscopy.[51] This will provide more objective assessment of the underlying disease profile, perhaps at the level of the individual patient, to aid in clinical management of patients with AAU. For example, the metabolic composition of the AqH may in the future reclassify patients into distinct treatment groups to improve risk assessment and prognosis.

Uric acid levels were consistently higher in patients with B27-AAU. Although we did not observe a correlation between uric acid levels and anterior chamber cell count, its role in inflammation requires further attention. Uric acid can act as a danger signal by activation of the nucleotide-binding oligomerization domain–like receptor P3 inflammasome[52] in macrophages and CD11c-positive dendritic cells.[53] Interestingly, CD11c-positive dendritic cells have recently been found to be enriched in the AqH of patients with noninfectious AAU.[54] However, because uric acid may also function as an anti-inflammatory antioxidant, future studies are needed to establish the role of uric acid in the pathogenesis of B27-AAU.[52,55]

The outcomes of this study need to be considered in light of the following limitations. Metabolomics may provide a powerful tool to interrogate the metabolic machinery underlying eye disease, but the use of untargeted MS requires the careful design of strategies that maximize signal-to-noise ratio, minimize unambiguous annotation, and ensure robustness of the identified peaks.[56–58] DIMS is able to perform MS acquisition without previous chromatographic separation, which results in fast measurements on low sample volumes, making it a useful tool for untargeted, hypothesis-generating approaches.[59,60] However, metabolites with a similar mass share peaks, which may lead to ambiguous annotation of DIMS spectra (like 4-methyl-2-oxopentanoate [ie, ketoleucine] and 3-methyl-2-oxopentanoate).[14] To overcome this challenge, we followed a top-down untargeted design to prioritize spectra of peaks for detailed and standard controlled technical and biological replication, here standard controlled LC-MS/MS for short-chain fatty acids. This analysis confirmed the increased intensity of 4-methyl-

2-oxopentanoate (ie, ketoleucine, over 3-methyl-2-oxopentanoate) in B27-AAU. However, other overlapping peaks might have hampered detection of correlation between DIMS and LC-MS/MS data for several metabolites.

In addition, the identified pathways are based on PLS-DA models of the metabolic profiles. PLS-DA is a standard multivariate classification algorithm that is widely used within the metabolomics field because of its sufficient handling of collinearity and noise while at the same time conveniently summarizing the classification potential of individual metabolites into a VIP score that aids in prioritizing metabolites for further analysis. However, regression models including PLS-DA are prone to overfitting.[61] To minimize the technical and statistical limitations of PLS-DA models, we followed a study design based on independent detection platforms and independent patient cohorts.[62] The need for such stringent criteria is clearly demonstrated by the number of validated metabolites across all 3 runs—an approach that is not commonly exploited in ocular fluid studies.

Finally, the patient cohorts were not matched in sex, age, treatment, sample storage time, or uveitis activity because ocular fluid collection is restricted to AqH taps for diagnostic purposes or surgery. This resulted in different storage times of the samples between the 2 uveitis groups. However, most metabolites are stable at −80°C, including ascorbic acid and leucine.[63,64] Also, we observed no correlation between ketoleucine and storage time (Supplemental Figure 4; Supplemental Material available at AJO.com). We also did not observe an association between age or sex and ascorbic acid and ketoleucine. Treatment regimens were not very different between the 2 uveitis groups (Table 1); we believe that the effect of therapy in this study was minimal. However, additional factors affecting metabolic status, such as diet or smoking, were not taken into account. We believe, however, that the independent biological replication, using 2 patient cohorts, has substantially decreased bias from such unaccounted factors.

In summary, our results show that patients with B27-AAU have a distinct metabolic profile in their AqH compared with patients with idiopathic AAU. This metabolic profile is characterized by changes in BCAA synthesis, ascorbate metabolism, and the TCA cycle, in particular the elevated metabolic compound ketoleucine, which correlated with disease activity in patients with B27-AAU.

FUNDING/SUPPORT: THIS STUDY WAS SUPPORTED BY UNRESTRICTED GRANTS FROM THE DR. F.P. FISCHER STICHTING AND THE Landelijke Stichting voor Blinden en Slechtzienden. The funders had no role in study design, data collection and analysis, decision to publish, or preparation of the manuscript. Financial Disclosures: The following authors have no financial disclosures: Fleurieke H. Verhagen, Edwin C.A. Stigter, Mia L. Pras-Raves, Boudewijn M.T. Burgering, Saskia M. Imhof, Timothy R.D.J. Radstake, Joke H. de Boer, and Jonas J.W. Kuiper. All authors attest that they meet the current ICMJE criteria for authorship.

Other Acknowledgments: We thank Marcel Willemsen (University Medical Center Utrecht) and Nagore Del Rio Ibisate (Universidad de Oviedo) for technical and logistic support.

REFERENCES

1. Bajwa A, Osmanzada D, Osmanzada S, et al. Epidemiology of uveitis in the mid-Atlantic United States. *Clin Ophthalmol* 2015;9:889–901.
2. Mercanti A, Parolini B, Bonora A, Lequaglie Q, Tomazzoli L. Epidemiology of endogenous uveitis in north-eastern Italy. Analysis of 655 new cases. *Acta Ophthalmol Scand* 2001;79(1):64–68.
3. Llorenç V, Mesquida M, Sainz de la Maza M, et al. Epidemiology of uveitis in a Western urban multiethnic population. The challenge of globalization. *Acta Ophthalmol* 2015;93(6):561–567.
4. Verhagen FH, Brouwer AH, Kuiper JJW, Ossewaarde-van Norel J, ten Dam-van Loon NH, de Boer JH. Potential predictors of poor visual outcome in human leukocyte antigen-B27–associated uveitis. *Am J Ophthalmol* 2016;165(165):179–187.
5. Power WJ, Rodriguez A, Pedroza-Seres M, Foster CS. Outcomes in anterior uveitis associated with the HLA-B27 haplotype. *Ophthalmology* 1998;105(9):1646–1651.
6. Chang JH, McCluskey PJ, Wakefield D. Acute anterior uveitis and HLA-B27. *Surv Ophthalmol* 2005;50(4):364–388.
7. Khan MA, Haroon M, Rosenbaum JT. Acute anterior uveitis and spondyloarthritis: more than meets the eye. *Curr Rheumatol Rep* 2015;17(9):59.
8. Zhao B, Chen W, Jiang R, et al. Expression profile of IL-1 family cytokines in aqueous humor and sera of patients with HLA-B27 associated anterior uveitis and idiopathic anterior uveitis. *Exp Eye Res* 2015;138:80–86.
9. Chen W, Zhao B, Jiang R, et al. Cytokine expression profile in aqueous humor and sera of patients with acute anterior uveitis. *Curr Mol Med* 2015;15(6):543–549.
10. Milne SB, Mathews TP, Myers DS, Ivanova PT, Brown HA. Sum of the parts: mass spectrometry-based metabolomics. *Biochemistry* 2013;52(22):3829–3840.
11. Guo J, Yan T, Bi H, et al. Plasma metabonomics study of the patients with acute anterior uveitis based on ultra-performance liquid chromatography-mass spectrometry. *Graefes Arch Clin Exp Ophthalmol* 2014;252(6):925–934.
12. Young SP, Nessim M, Falciani F, et al. Metabolomic analysis of human vitreous humor differentiates ocular inflammatory disease. *Mol Vis* 2009;15:1210–1217.
13. Zhang T, Zhang A, Qiu S, Yang S, Wang X. Current trends and innovations in bioanalytical techniques of metabolomics. *Crit Rev Anal Chem* 2016;46(4):342–351.
14. Lísa M, Cífková E, Khalikova M, Ovčačíková M, Holčapek M. Lipidomic analysis of biological samples: comparison of liquid chromatography, supercritical fluid chromatography and direct infusion mass spectrometry methods. *J Chromatogr A* 2017;1525:96–108.

15. Ramos RJ, Pras-Raves ML, Gerrits J, et al. Vitamin B6 is essential for serine de novo biosynthesis. *J Inherit Metab Dis* 2017;40(6):883–891.
16. Xia J, Psychogios N, Young N, Wishart DS. MetaboAnalyst: a web server for metabolomic data analysis and interpretation. *Nucleic Acids Res* 2009;37(Web Server issue): W652–W660.
17. Xia J, Wishart DS. Using MetaboAnalyst 3.0 for comprehensive metabolomics data analysis. In: Current Protocols in Bioinformatics. Vol 55. Hoboken, NJ, USA: John Wiley & Sons, Inc.; 2016:14.10.1-14.10.91.
18. Jabs DA, Nussenblatt RB, Rosenbaum JT. Standardization of uveitis nomenclature for reporting clinical data. Results of the First International Workshop. *Am J Ophthalmol* 2005; 140(3):509–516.
19. Brosnan JT, Brosnan ME. Branched-chain amino acids: enzyme and substrate regulation. *J Nutr* 2006;136(1 suppl): 207S–211S.
20. Rosenbaum JT, McDevitt HO, Guss RB, Egbert PR. Endotoxin-induced uveitis in rats as a model for human disease. *Nature* 1980;286(5773):611–613.
21. Mérida S, Palacios E, Navea A, Bosch-Morell F. Macrophages and uveitis in experimental animal models. *Mediators Inflamm* 2015;2015:1–10.
22. Papathanassiu AE, Ko J-H, Imprialou M, et al. BCAT1 controls metabolic reprogramming in activated human macrophages and is associated with inflammatory diseases. *Nat Commun* 2017;8(May):16040.
23. Robinson PC, Claushuis TAM, Cortes A, et al. Genetic dissection of acute anterior uveitis reveals similarities and differences in associations observed with ankylosing spondylitis. *Arthritis Rheumatol* 2015;67(1):140–151.
24. Rosenbaum JT. Evolving "diagnostic" criteria for axial spondyloarthritis in the context of anterior uveitis. *Ocul Immunol Inflamm* 2016;24(4):445–449.
25. Wang W, Yang G-J, Zhang J, et al. Plasma, urine and ligament tissue metabolite profiling reveals potential biomarkers of ankylosing spondylitis using NMR-based metabolic profiles. *Arthritis Res Ther* 2016;18(1):244.
26. Jiang M, Chen T, Feng H, et al. Serum metabolic signatures of four types of human arthritis. *J Proteome Res* 2013;12(8): 3769–3779.
27. Lin P, Bach M, Asquith M, et al. HLA-B27 and human β2-microglobulin affect the gut microbiota of transgenic rats. *PLoS One* 2014;9(8):e105684.
28. Asquith MJ, Stauffer P, Davin S, Mitchell C, Lin P, Rosenbaum JT. Perturbed mucosal immunity and dysbiosis accompany clinical disease in a rat model of spondyloarthritis. *Arthritis Rheumatol* 2016;68(9):2151–2162.
29. Shoaie S, Ghaffari P, Kovatcheva-Datchary P, et al. Quantifying diet-induced metabolic changes of the human gut microbiome. *Cell Metab* 2015;22(2):320–331.
30. Shao T-J, He Z-X, Xie Z-J, Li H-C, Wang M-J, Wen C-P. Characterization of ankylosing spondylitis and rheumatoid arthritis using 1H NMR-based metabolomics of human fecal extracts. *Metabolomics* 2016;12(4):1–8.
31. Kasper M, Gabriel D, Möller M, et al. Novel everolimus-loaded nanocarriers for topical treatment of murine experimental autoimmune uveoretinitis (EAU). *Exp Eye Res* 2018;168:49–56.
32. Blair J, Barry R, Moore DJ, Denniston AK. A comprehensive review of mTOR-inhibiting pharmacotherapy for the treatment of non-infectious uveitis. *Curr Pharm Des* 2017; 23(20):3005–3014.
33. Wolfson RL, Chantranupong L, Saxton RA, et al. Sestrin2 is a leucine sensor for the mTORC1 pathway. *Science* 2016; 351(6268):43–48.
34. Ananieva EA, Patel CH, Drake CH, Powell JD, Hutson SM. Cytosolic branched chain aminotransferase (BCATc) regulates mTORC1 signaling and glycolytic metabolism in CD4+ T cells. *J Biol Chem* 2014;289(27):18793–18804.
35. Jha AK, Huang SCC, Sergushichev A, et al. Network integration of parallel metabolic and transcriptional data reveals metabolic modules that regulate macrophage polarization. *Immunity* 2015;42(3):419–430.
36. O'Neill LAJ. A broken Krebs cycle in macrophages. *Immunity* 2015;42(3):393–394.
37. Mohammed BM, Fisher BJ, Kraskauskas D, et al. Vitamin C: a novel regulator of neutrophil extracellular trap formation. *Nutrients* 2013;5(8):3131–3151.
38. Tan PH, Sagoo P, Chan C, et al. Inhibition of NF-kappa B and oxidative pathways in human dendritic cells by antioxidative vitamins generates regulatory T cells. *J Immunol* 2005; 174(12):7633–7644.
39. Williams RN, Paterson CA. The influence of topical corticosteroid therapy upon polymorphonuclear leukocyte distribution, vascular integrity and ascorbate levels in endotoxin-induced inflammation of the rabbit eye. *Exp Eye Res* 1987; 44(2):191–198.
40. Dick AD, Siepmann K, Dees C, et al. Fas-Fas ligand-mediated apoptosis within aqueous during idiopathic acute anterior uveitis. *Invest Ophthalmol Vis Sci* 1999;40(10):2258–2267.
41. Rose-Nussbaumer J, Li Y, Lin P, et al. Aqueous cell differentiation in anterior uveitis using fourier-domain optical coherence tomography. *Investig Ophthalmol Vis Sci* 2015;56(3):1430–1436.
42. Chi Z-L, Hayasaka Y, Zhang X-Y, Cui H-S, Hayasaka S. S100A9-positive granulocytes and monocytes in lipopolysaccharide-induced anterior ocular inflammation. *Exp Eye Res* 2007;84(2):254–265.
43. Agrawal R, Keane PA, Singh J, Saihan Z, Kontos A, Pavesio CE. Comparative analysis of anterior chamber flare grading between clinicians with different levels of experience and semi-automated laser flare photometry. *Ocul Immunol Inflamm* 2016;24(2):184–193.
44. Invernizzi A, Marchi S, Aldigeri R, et al. Objective quantification of anterior chamber inflammation: measuring cells and flare by anterior segment optical coherence tomography. *Ophthalmology* 2017;124(11):1670–1677.
45. Rhee SY, Jung ES, Park HM, et al. Plasma glutamine and glutamic acid are potential biomarkers for predicting diabetic retinopathy. *Metabolomics* 2018;14(7):89.
46. Pietrowska K, Dmuchowska DA, Krasnicki P, et al. An exploratory LC-MS-based metabolomics study reveals differences in aqueous humor composition between diabetic and non-diabetic patients with cataract. *Electrophoresis* 2018; 39(9-10):1233–1240.
47. Laíns I, Kelly RS, Miller JB, et al. Human plasma metabolomics study across all stages of age-related macular degeneration identifies potential lipid biomarkers. *Ophthalmology* 2018;125(2):245–254.

48. Park KS, Xu CL, Cui X, Tsang SH. Reprogramming the metabolome rescues retinal degeneration. *Cell Mol Life Sci* 2018;75(9):1559–1566.
49. Barbosa-Breda J, Himmelreich U, Ghesquière B, Rocha-Sousa A, Stalmans I. Clinical metabolomics and glaucoma. *Ophthalmic Res* 2018;59(1):1–6.
50. Pietrowska K, Dmuchowska DA, Krasnicki P, Mariak Z, Kretowski A, Ciborowski M. Analysis of pharmaceuticals and small molecules in aqueous humor. *J Pharm Biomed Anal* 2018;159:23–36.
51. Sideroudi T, Pharmakakis N, Tyrovolas A, Papatheodorou G, Chryssikos GD, Voyiatzis GA. Non-contact detection of ciprofloxacin in a model anterior chamber using Raman spectroscopy. *J Biomed Opt* 2007;12(3):34005.
52. El Ridi R, Tallima H. Physiological functions and pathogenic potential of uric acid: a review. *J Adv Res* 2017;8(5):487–493.
53. Kool M, Soullié T, van Nimwegen M, et al. Alum adjuvant boosts adaptive immunity by inducing uric acid and activating inflammatory dendritic cells. *J Exp Med* 2008;205(4):869–882.
54. O'Rourke M, Fearon U, Sweeney CM, et al. The pathogenic role of dendritic cells in non-infectious anterior uveitis. *Exp Eye Res* 2018;173:121–128.
55. Ames BN, Cathcart R, Schwiers E, Hochstein P. Uric acid provides an antioxidant defense in humans against oxidant- and radical-caused aging and cancer: a hypothesis. *Proc Natl Acad Sci U S A* 1981;78(11):6858–6862.
56. Tan SZ, Begley P, Mullard G, Hollywood KA, Bishop PN. Introduction to metabolomics and its applications in ophthalmology. *Eye* 2016;30(6):773–783.
57. Frédérich M, Pirotte B, Fillet M, De Tullio P. Metabolomics as a challenging approach for medicinal chemistry and personalized medicine. *J Med Chem* 2016;59(19):8649–8666.
58. Mahieu NG, Patti GJ. Systems-level annotation of a metabolomics data set reduces 25 000 features to fewer than 1000 unique metabolites. *Anal Chem* 2017;89(19):10397–10406.
59. Castrillo JI, Hayes A, Mohammed S, Gaskell SJ, Oliver SG. An optimized protocol for metabolome analysis in yeast using direct infusion electrospray mass spectrometry. *Phytochemistry* 2003;62(6):929–937.
60. Beckmann M, Parker D, Enot DP, Duval E, Draper J. High-throughput, nontargeted metabolite fingerprinting using nominal mass flow injection electrospray mass spectrometry. *Nat Protoc* 2008;3(3):486–504.
61. Gromski PS, Muhamadali H, Ellis DI, et al. A tutorial review: metabolomics and partial least squares-discriminant analysis—a marriage of convenience or a shotgun wedding. *Anal Chim Acta* 2015;879:10–23.
62. Mischak H, Allmaier G, Apweiler R, et al. Recommendations for biomarker identification and qualification in clinical proteomics. *Sci Transl Med* 2010;2(46):46ps42.
63. Haid M, Muschet C, Wahl S, et al. Long-term stability of human plasma metabolites during storage at −80°C. *J Proteome Res* 2018;17(1):203–211.
64. Jenab M, Bingham S, Ferrari P, et al. Long-term cryoconservation and stability of vitamin C in serum samples of the European prospective investigation into cancer and nutrition. *Cancer Epidemiol Biomarkers Prev* 2005;14(7):1837–1840.